

2022

Experimental Investigation of Liquid Slugging in the Suction Mufflers of Hermetic Reciprocating Compressors

Teo B Balconi

Tadeu T Rodrigues

Cesar J Deschamps

Follow this and additional works at: <https://docs.lib.purdue.edu/icec>

Balconi, Teo B; Rodrigues, Tadeu T; and Deschamps, Cesar J, "Experimental Investigation of Liquid Slugging in the Suction Mufflers of Hermetic Reciprocating Compressors" (2022). *International Compressor Engineering Conference*. Paper 2744.
<https://docs.lib.purdue.edu/icec/2744>

This document has been made available through Purdue e-Pubs, a service of the Purdue University Libraries. Please contact epubs@purdue.edu for additional information. Complete proceedings may be acquired in print and on CD-ROM directly from the Ray W. Herrick Laboratories at <https://engineering.purdue.edu/Herrick/Events/orderlit.html>

Experimental Investigation of Liquid Slugging in the Suction Mufflers of Hermetic Reciprocating Compressors

Teo B BALCONI¹, Tadeu T RODRIGUES², Cesar J DESCHAMPS^{1*}

¹POLO Research Laboratories for Emerging Technologies in Cooling and Thermophysics
Department of Mechanical Engineering, Federal University of Santa Catarina
88040900 Florianopolis, SC, Brazil

²NIDEC-GA, R&D,
Joinville, SC, Brazil

* Corresponding Author: deschamps@polo.ufsc.br

ABSTRACT

Compressor liquid slugging occurs when liquid refrigerant, lubricant oil, or a mixture of both reach the compression chamber. This phenomenon is detrimental to reciprocating compressors because it can damage valves and other components. This paper reports an experimental investigation of oil flow in a simplified geometry of suction muffler of small reciprocating compressor, aiming to quantify the volume of liquid that reaches the compression chamber after a liquid slugging event. A test bench was developed to measure the volume of oil that reaches the muffler outlet after the injection of a known volume, being comprised of three main components: calorimeter, liquid injection system and test section. The superheated gas cycle calorimeter was used to submit the muffler to specified values of pressure and temperature. The injection system consists of a reservoir of oil under controlled pressure, supply line and a solenoid valve that controls the injections into the test section. The test section is formed by a container with a sight glass where the transparent muffler made of acrylic is inserted. A high-speed camera is placed in front of the sight glass to allow observation of the flow of oil through the muffler. Measurements under different injection pressures showed that the phenomenon of liquid slugging is quite random and that the volume of liquid reaching the muffler outlet increases with the injection velocity.

1. INTRODUCTION

In refrigeration systems, refrigerant fluid coexists in vapor, liquid, and two-phase forms. In addition, there is also the circulation of oil in the system and, in greater quantity, inside the compressor. According to Youbi-Idrissi and Bonjour (2008), the oil circulation rate (OCR) tends to remain fixed, being slightly higher for POE oils in comparison with mineral oils. It is well known that solubility between oil and refrigerant increases with pressure and decreases with temperature (Bell et al., 2013). Hence, the mass fraction of refrigerant dissolved in the oil increases when the compressor is switched off because the temperature decreases and the pressure increases. When the compressor is switched on, the sudden pressure drop inside the compressor shell super saturates the refrigerant-oil mixture and foam is formed (Fortkamp and Barbosa, 2015).

Naturally, compressors are designed to operate only with vapor in the compression chamber. In the presence of liquid refrigerant or oil, the pressure in the compression chamber can reach values 10 times higher than the pressure in discharge chamber (Singh, R. et al., 1986). This can generate excessive stresses and strains in the connecting rod-crank mechanism, valve plate and valves, leading to compressor failure (Laughman et al., 2006). For example, Stoupe and Lau (1989) surveyed the causes of reciprocating compressor failures in air conditioning systems and found that 20% of the failures were caused by liquid slugging. According to Liu and Soedel (1995), reciprocating compressors are very vulnerable to liquid slugging.

The admission of liquid can occur at the compressor startup, known as flooded start, and during the compressor operation. The causes for the admission of oil are the return of oil circulating in the system (OCR) and due to the foaming phenomenon during the compressor startup. On the other hand, the admission of liquid refrigerant can occur

due to several factors: (i) excessive refrigerant charge in the system, (ii) very long compressor off periods, (iii) operation in very low temperature environments, (iv) partial evaporation of the refrigerant due to low thermal loads, failure of forced ventilation, among others, and (v) use of hot gas defrost.

Few studies in the literature address the admission of liquid into the compression chamber of small reciprocating compressors. This type of compressor adopts suction mufflers to attenuate the noise generated by the pressure pulsation in the flow brought about by the reciprocal movement of the piston. Due to the complexity of the flow inside the suction muffler, its effect on the amount of liquid that reaches the compression chamber during a liquid slugging event is not known. There is even the question of whether liquid admitted into the suction system can reach the compression chamber. Bianchi et al. (2021) numerically simulated the injection of oil in a simplified suction muffler geometry of a compressor operating with R134a, aimed at predicting the ratio between the volume of oil entering and exiting the muffler. An experimental bench was also developed to investigate injections of 16 ml of POE ISO 22 oil at three velocities. Good agreement between the experimental and numerical results was found for the tests under high injection velocities. Despite the random character of the phenomenon, the authors found that the volume of liquid reaching the exit of the muffler increases with the velocity of the jet at the entrance.

This paper reports an experimental investigation of the flow of lubricating oil in a simplified suction muffler geometry brought about by the injection of oil at different velocities. The volume of oil collected at the outlet of the muffler is measured and a high-speed camera shows the flow of oil inside the muffler. The analysis also considers the effect the refrigerant dissolved in the oil has on the on the flow inside the muffler.

2. EXPERIMENTAL SETUP AND PROCEDURE

2.1 Test bench

A test bench was developed to measure the volume of oil that reaches the muffler outlet after the injection of a known volume of oil at the muffler entrance. The test bench operates in combination with a hot cycle calorimeter to submit the suction muffler to specified values of pressure and temperature. As shown in Figure 1, the test bench is formed by a small reciprocating compressor (C), two electric resistances (EH), two oil separators (OS), a refrigerant buffer (RB), a suction control valve (SV), a discharge control valve (DV), temperature (T) and pressure (P) sensors, solenoid valves (S), and the test section (TS) where the muffler is placed in series with the compressor.

Figure 2 shows the corresponding p-h diagram for this arrangement defined by the points (1, 2, a, b, c, d) also indicated in the test bench (Figure 1). The operating condition is set by the controlling the valves SV and DV and the thermal resistances EH, which also keeps the cycle in the superheated vapor region. The oil separator OS after the test section prevents the tested oil from reaching the compressor, while the oil separator downstream of the compressor ensures that the oil from the compressor itself is collected and returned to its sump. Solenoid valves (S) allow the control of the flow through the test section, which is necessary to measure the volume of oil collected at the muffler outlet.

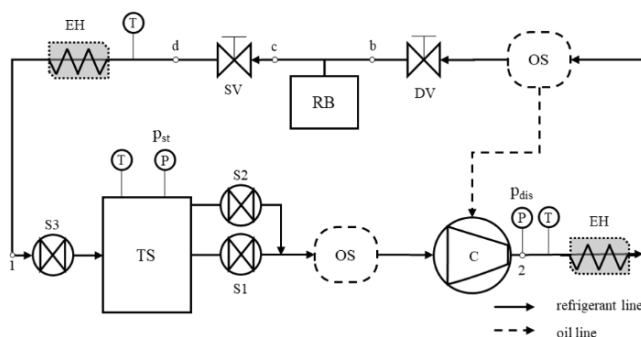


Figure 1: Schematic of the test bench.

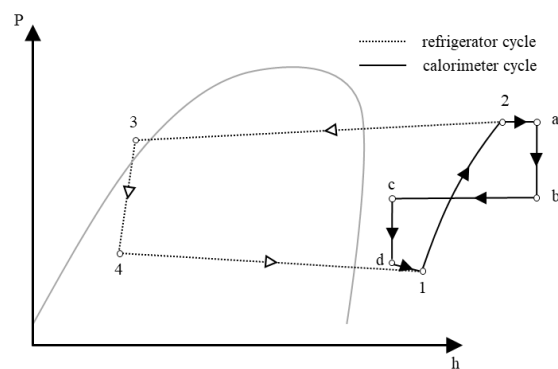


Figure 2: p-h diagram associated with the hot-cycle calorimeter and refrigeration cycle.

The overall layout of the test bench in Figure 3 indicates the auxiliary line responsible for the oil injection. The injection system consists of a reservoir of oil under controlled pressure, oil supply line and a solenoid valve that controls the injection of oil into the test section. A gear pump (IP) takes oil from the reservoir (OR) to the oil injector (OI) where the volume of oil to be injected is measured. The line (OIEL) guarantees the pressure equalization between the reservoirs OR and OI and the gear pump driven by a stepper motor can circulate the oil in both directions. The solenoid valves S4 and S5 are used to open and close these lines quickly. A micrometer control valve (OPV) allows the oil in the injector to be set to the intermediate pressure (section b-c in the Figure 2). The reservoir OB is used to ensure that the pressure is maintained during the injection, which is carried out by opening the solenoid valve S6. The injected oil needs to be collected and returned from the test section (TS) to the oil reservoir (OR). A second gear pump (RP) performs this task through the return line (ORL) with the assistance of the equalization line (OREL). Both lines have manual globe valves (GV). A third globe valve (GV) allows the removal of dissolved refrigerant fluid from the oil with the assistance of a vacuum pump.

2.2 Suction muffler and test section

Figure 4 shows the actual suction muffler and corresponding simplified geometry adopted in the present study, following Rodrigues (2018). The test section is formed by a container with a sight glass where the transparent muffler made of acrylic is inserted (Figure 5). A high-speed camera is placed in front of the sight glass to allow observation of the flow through the muffler. As shown in Figure 3, the test section is positioned in the hot-cycle calorimeter circuit, before the compressor suction line, so that the whole container is under the selected suction pressure condition of the compressor. A positioning system supports the collector block and adjusts the suction muffler inlet concentrically to the injection tube and 20 mm apart, as seen in Figure 5(a). The oil return system shown in Figure 5(b) is formed by an oil sump, a built-in gear pump (RP), a stepper motor and an outlet orifice through which the oil is directed to the reservoir (OR).

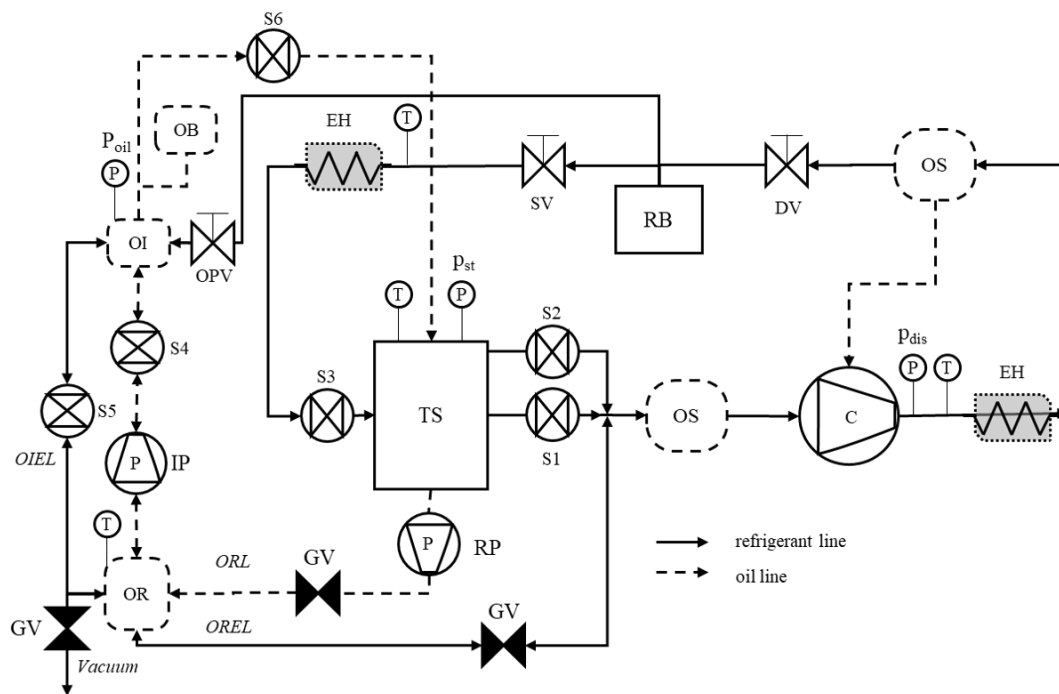


Figure 3: Overall representation of the test section.

2.3 Test procedure

The tests were carried out with the following procedure: (i) the test bench is set under the specified operating condition: $T_e = -23.3^\circ\text{C}$ ($p_e = 1.15$ bar), $T_c = 10.4^\circ\text{C}$ ($p_c = 4.21$ bar), $T_{is} = 25^\circ\text{C}$ and the compressor speed = 3000 rpm; (ii) the oil from the reservoir (OR) is transported to the injector (OI) where its volume is measured; (iii) the OPV micrometric valve controlled by a stepper motor and connected to the intermediate refrigerant fluid reservoir (RB) allows the adjustment of the injection pressure; (iv) the solenoid valve S6 is opened and the injection of oil is carried out for 2 seconds to empty the injector tube, with the high-speed camera activated; (v) the compressor is kept running for 60

seconds and then switched off; (vi) the collected volume of oil is recorded by a regular camera; (vii) after a few injections, the collect oil is returned to the reservoir (OR). It should be mentioned that the measurements were carried out for pure oil and with a mixture of refrigerant dissolved in the oil. In first case, vacuum was carried out in the reservoir (OR) until the refrigerant was fully removed, whereas in the second case both fluids were kept in contact for 24 hours.

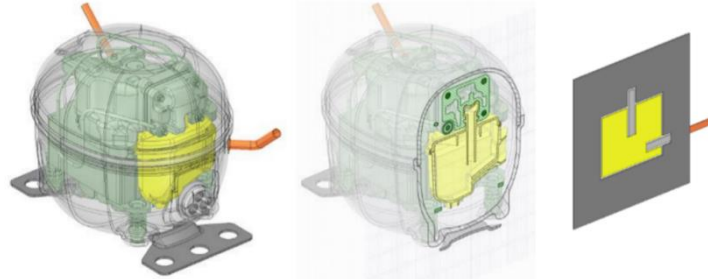


Figure 4: Simplified suction muffler geometry (Rodrigues, 2018).

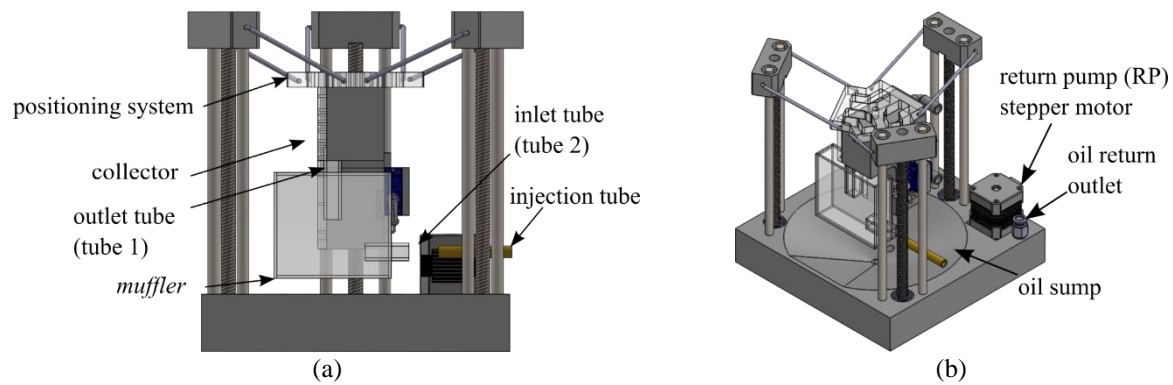


Figure 5: Test section. (a) front view; (b) isometric view.

2.4 Indirect measurements

The measurements of the collected volume and injection velocity were indirect. The volume was calculated from the height of the liquid column, made available by an image processing software, multiplied by the known collector cross-sectional area. The injection velocity was estimated as the ratio between the distance L traveled by the liquid and the corresponding time interval, estimated from high-speed footage. The cross-sectional area (A) of the oil collector was calculated from measurements of its width with a Mitutoyo 145-185 inner micrometer and depth with a Mitutoyo 530-312 caliper. The distance L used to calculate the jet velocity was also measured with the caliper. A total of 30 repetitions were performed to obtain the mean value of each dimension.

2.5 Measurement uncertainty

The Shapiro-Wilk and Anderson-Darling normality tests were applied to the measurements and their uncertainties were estimated following Montgomery and Runger (2018). The temperature was measured with a thermocouple Omega TT-T-24-SLE (accuracy ± 0.5 °C) and the pressure was measured with a piezoresistive Velki VKP-011 (accuracy $\pm 0.25\%$ of span). The accuracy of these sensors was used to compose the measurement uncertainty U , as

$$U = u_c \cdot t \quad (2)$$

where t is the t-student coefficient for a confidence level of 95% and u_c is the combined uncertainty obtained from

$$u_c^2 = u_m^2 + \left(\frac{S}{\sqrt{n}}\right)^2 \quad (1)$$

where u_m , S and n are measurement uncertainty, sample standard deviation and number of samples respectively.

3. RESULTS

Two groups of tests were performed. The first adopted pure oil and nominal injection pressures (Δp_{inj}) of 0.8 bar (Test 1), 1.0 bar (Test 2), 1.2 bar (Test 3), 1.5 bar (Test 4) and 2.0 bar (Test 5) with 9 repetitions each. The second group considered dissolved refrigerant in the oil and nominal injection pressures of 1.5 bar (Test 6) and 2.0 bar (Test 7) with 12 repetitions each. The volume of oil injected in all tests was set to 16 ml. The normality condition was verified for the samples of collected volumes and injection velocities and only the injection velocity for test 7 was not successful. The average values and the expanded uncertainty of the operating conditions are indicated in the Table 1. The analysis of the results to be presented next considered the tests with pure oil and tests with refrigerant dissolved in the oil. In addition to that, the measurements discussed herein are also compared with the experimental and numerical results obtained by Bianchi et al. (2021).

Table 1: Operation conditions means and expanded uncertainty

Tests	Δp_{inj} [bar]		p_{dis} [bar]		p_{suc} [bar]		T_{ts} [°C]	
	ref: 0.8/1/1.2/1.5/2		ref: 4.21		ref: 1.15		ref: 25	
	mean	U	mean	U	mean	U	mean	U
Test 1	0.851	± 0.057	4.154	± 0.092	1.131	± 0.057	24.94	± 1.13
Test 2	1.033	± 0.057	4.114	± 0.095	1.120	± 0.057	24.91	± 1.13
Test 3	1.240	± 0.057	4.185	± 0.095	1.128	± 0.057	24.81	± 1.14
Test 4	1.604	± 0.057	4.087	± 0.091	1.118	± 0.057	25.10	± 1.14
Test 5	2.102	± 0.057	4.048	± 0.092	1.107	± 0.057	25.80	± 1.14
Test 6	1.606	± 0.056	4.151	± 0.088	1.135	± 0.055	25.58	± 1.11
Test 7	2.109	± 0.055	4.131	± 0.088	1.132	± 0.055	25.95	± 1.10

3.1 Pure oil

The results for injection velocity and collected volume of pure oil are shown in Table 2, as well as the corresponding expanded uncertainties U and standard deviations S . The high standard deviations are associated with the random character of the phenomenon. Table 2 also shows that there is an approximate linear relationship between the injection velocity and the injection pressure.

Figure 6 shows results for the collected volume of oil as a function of the injection velocity. As can be observed, there is a strong increase in the collected volume when the injection velocity is changed from 3.82 to 4.67 m/s (tests 1 and 2), followed by much smaller increases when the injection velocity is varied from 4.67 to 7.92 m/s (tests 2 and 5). These results suggest different flow dynamics inside the suction muffler according to the injection velocity.

Table 2: Injection velocity and collected volume for pure oil.

	Δp_{inj} [bar]	velocity [m/s]		V_{col} [ml]			
		mean	U	mean	U	S	S/ V_{col}
		Test 1	0.8	3.82	± 0.34	0.062	± 0.029
Test 2	1.0	4.67	± 0.30	0.119	± 0.052	0.067	56%
Test 3	1.2	5.56	± 0.27	0.126	± 0.067	0.087	69%
Test 4	1.5	6.83	± 0.63	0.133	± 0.055	0.072	54%
Test 5	2.0	7.92	± 0.52	0.148	± 0.032	0.042	28%

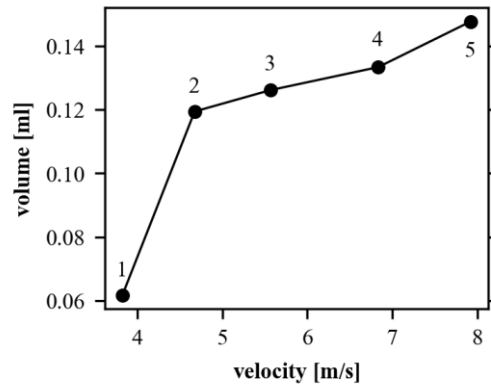


Figure 6: Collected volume of oil as a function of the injection velocity.

3.2 Refrigerant dissolved in the oil

To assess the influence of refrigerant dissolved in the oil on the collected volume, nominal operating conditions used for tests 4 and 5 were repeated, but this time using a saturated mixture of refrigerant and oil, and denoted as tests 6 and 7. Table 3 shows the presence of refrigerant brings about higher injection velocities. This was expected since the viscosity of the mixture is smaller than that of the pure oil. As a consequence, greater volumes of liquid are collected.

Figure 7 shows the mean values of the collected volumes and the expanded uncertainties, whereas Figure 8 presents the corresponding standard deviations, which are similar for tests with pure oil and with refrigerant dissolved in the oil. It seems the refrigerant solubilized in the oil acts to increase the collected volume of oil, as indicated by tests 5 and 6 with similar injection velocities. The p-value of the unpaired equal variance T-test one-tail is 0.00177 and hence, from the statistical point of view with 0.01 level of significance (α), one can conclude that this effect of the dissolved refrigerant in the oil is true.

Table 3: Injection velocity and collected volume for mixture of refrigerant and oil.

	Δp_{inj} [bar]	velocity [m/s]		V_{col} [ml]			
		mean	U	mean	U	S	S/ V_{col}
Test 6	1.5	7.42	± 0.31	0.212	± 0.029	0.045	21%
Test 7	2.0	8.81	± 0.34	0.273	± 0.032	0.050	18%

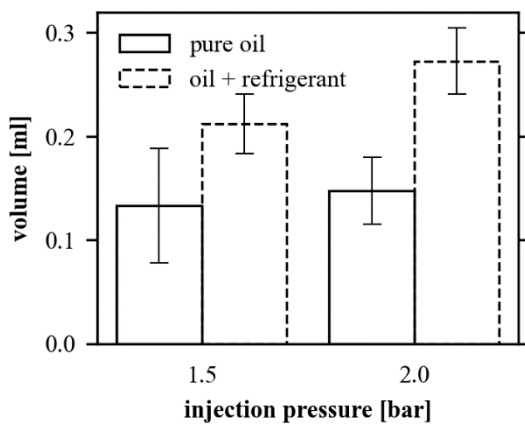


Figure 7: Collected volumes and expanded uncertainties for pure and solubilized oil.

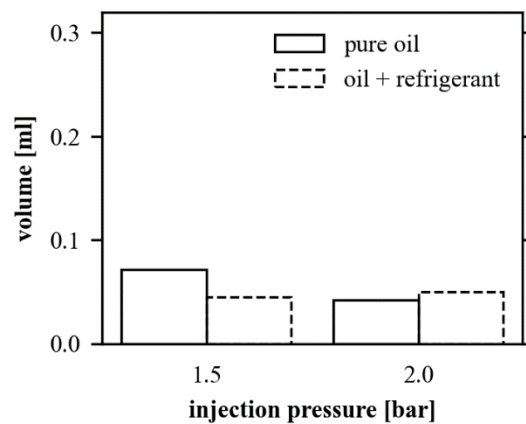


Figure 8: Standard deviations of collected volumes for pure and solubilized oil.

3.3 Comparison with results of other studies

Bianchi et al. (2021) performed an extensive numerical analysis of the oil injection in the same simplified geometry of suction muffler adopted herein, together with some measurements to validate the predictions of the simulation model. It should be mentioned that Bianchi et al. (2021) collected oil in a cumulative manner for several tests and estimated the volume of each test by subtracting the registered volumes of two consecutive tests. On the other hand, the measurements carried out in the present work were made after each test, with the collector system being then drained for a new test.

Table 4 shows that numerical and experimental results of Bianchi et al. (2021) for the tests 2 and 3 are close to the measurements of the present work, but the same is not observed for the test 1. However, it should be noted that predictions obtained by Bianchi et al. (2021) for test 1 is in closer agreement with the present measurement than with their experimental data. It can also be noted that the standard deviations of both experimental data are similar for the tests 2 and 3. However, Bianchi et al. (2021) found a much smaller standard deviation for small collected volumes (test 1) when compared with that of the present experimental procedure.

Table 4: Measurements of the present work and numerical and experimental results of Bianchi et al. (2021).

	Current work				Bianchi et al. (2021)				
					measurements				predictions
	V_{col} [ml]	U [ml]	S [ml]	S/V_{col} [%]	V_{col} [ml]	U [ml]	S [ml]	S/V_{col} [%]	value [ml]
Test 1	0.062	± 0.029	0.0381	62%	0.0124	± 0.0048	0.0062	50%	0.0732
Test 2	0.119	± 0.052	0.0673	56%	0.106	± 0.047	0.0611	58%	0.098
Test 3	0.126	± 0.067	0.0868	69%	0.149	± 0.048	0.0626	42%	0.144

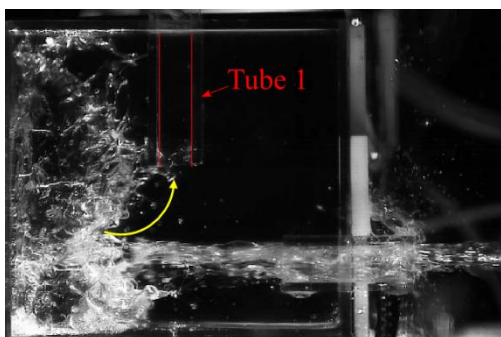
3.4 Flow dynamics in the suction muffler

The images registered by the high-speed camera (Figure 9) shows two mechanisms that help the injected oil to leave the suction muffler through the outlet tube (also indicated as tube 1 in Figure 5 and depicted by red lines in Figure 9). The most critical one occurs when the oil is injected and collides with the opposite wall, bouncing back towards the inlet of tube 1 and being directed to the muffler outlet. This mechanism shown in Figure 9(a) was identified as “high injection velocity”. In the second mechanism, referred hereafter as “low injection velocity”, the oil collides with the opposite wall and then splashes onto the upper left quadrant of the muffler, flowing along the wall towards the inlet of the tube 1, as illustrated in Figure 9(b).

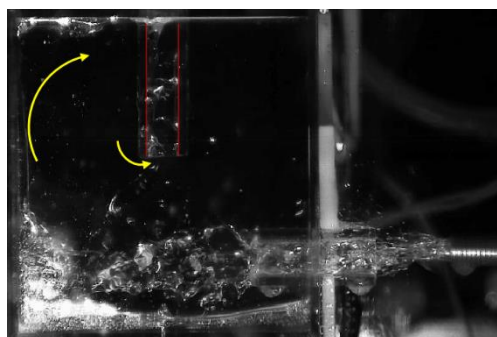
It is clear the injection velocity affects where the jet impinges onto the wall and the amount of oil exiting the muffler because of the resulting flow dynamics. Figure 9(c) shows that the jet at low velocities makes a downward trajectory and impinges on the lower region of the opposite wall. As the injection velocity increases, the jet trajectory becomes more and more straight, as illustrated in Figure 9(d). Naturally, the amount of oil exiting the suction muffler increases with the jet velocity since the resulting front of oil becomes closer to the entrance of the outlet tube. Nevertheless, as the jet velocity is increased further the location where the jet impacts against the wall eventually does not change further. In fact, this observation explains the difference observed between the results of tests 1 and 2 in Figure 6 regarding the collected volume as a function of the jet velocity.

After impinging on the opposite wall, the oil flow dynamics changes according to the injection velocity and the presence or not of refrigerant dissolved in the oil. Figure 9(e) shows that at low injection velocities (Test 1) the flow of oil inside the muffler is very little dispersed after reaching the wall. However, as depicted in Figure 9(f) for the condition of Test 5, the flow inside the muffler becomes more dispersed as the injection velocity is increased. If the velocity is further increased, as show in Figure 9(g) (Test 5), the flow becomes very dispersed and chaotic. This can explain the more gradual increase in the collected volume observed in Figure 6 when the injection velocity is changed from the condition of test 2 onwards. The refrigerant dissolved in the oil also acts to increase the flow dispersion inside the muffler, since the refrigerant lowers the superficial tension on the jet interface, which reduces the jet stability and anticipate its breakup. Figure 9(g) and Figure 9(h) show the flow inside the muffler for tests 4 and 6 with the same injection pressure of 1.5 bar, but without and with refrigerant dissolved in the oil, respectively. The presence of refrigerant in the oil gives rise to greater flow dispersion, in addition to the effects observed when the injection velocity

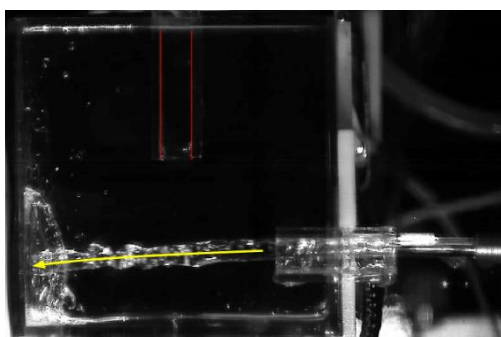
is increased. Therefore, the amount of oil exiting the muffler increases with the injection velocity and refrigerant dissolved in the oil.



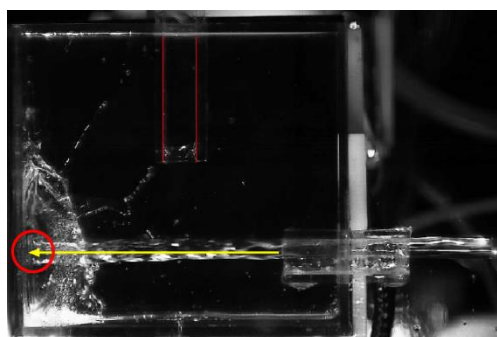
(a) High injection velocity.



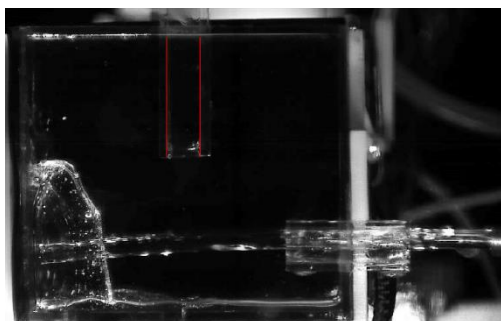
(b) Low injection velocity.



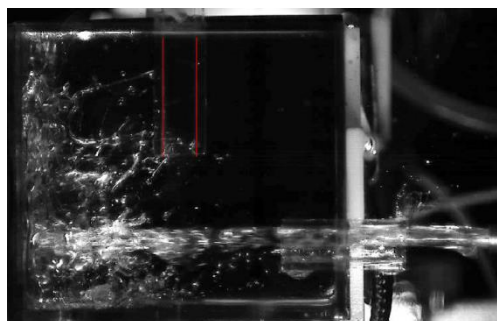
(c) Low injection velocity (Test 1).



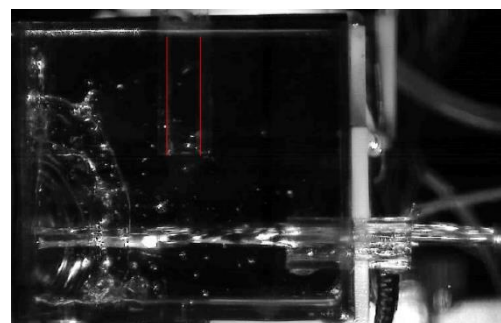
(d) Medium injection velocity (Test 3).



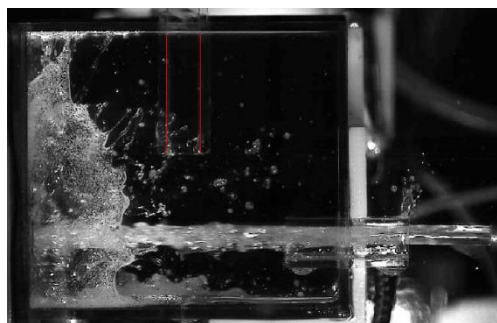
(e) Oil dispersion inside the muffler (Test 1).



(f) Oil dispersion inside the muffler (Test 5).



(g) Oil dispersion inside the muffler (Test 4).



(h) Oil dispersion inside the muffler (Test 6).

Figure 9: Collected volume of oil as a function of the injection velocity.

4. CONCLUSIONS

This paper reported an experimental investigation of oil flow in a simplified geometry of suction muffler of small reciprocating compressors, aiming to understand the phenomenon of liquid slugging. The tests showed a direct relationship between the injection velocity and the volume of oil exiting the muffler. There are two important mechanisms regarding the oil flow dynamics inside the muffler. The first occurs under high injection velocity in which the oil is directed to the outlet tube shortly after impinging on the opposite wall. The second takes place under low injection velocity in which the oil is dragged by the flow towards the outlet tube. We also found that the dispersion of the oil inside the muffler increases the amount of oil exiting the muffler, which is enhanced by the injection velocity and refrigerant dissolved in the oil.

NOMENCLATURE

n	number of measurements	[-]	V	volume	[ml]
p	pressure	[bar]	vel	velocity	[m/s]
S	sample standard deviation	[x]	Subscript		
T	temperature	[°C]	c	condensing	
t	t-student	[-]	col	collected	
U	expanded uncertainty	[x]	e	evaporating	
u _c	combined uncertainty	[x]	inj	injection	
u _m	measurement uncertainty	[x]	ts	test section	

REFERENCES

- Bell, I. H., Groll, E. A., Braun, J. E., & Horton, W. T. (2013). Experimental testing of an oil-flooded hermetic scroll compressor. *International Journal of Refrigeration*, 36(7), 1866–1873. <https://doi.org/10.1016/j.ijrefrig.2013.01.006>
- Bianchi, M., Deschamps, C. ~J., Rodrigues, T. ~T., & Paladino, E. ~E. (2021). Numerical-experimental investigation of liquid slugging in the suction muffler of a hermetic reciprocating compressor. *Materials Science and Engineering Conference Series*, 1180, 12017. <https://doi.org/10.1088/1757-899X/1180/1/012017>
- Fortkamp, F. P., & Barbosa, J. R. (2015). Refrigerant desorption and foaming in mixtures of HFC-134a and HFO-1234yf and a polyol ester lubricating oil. *International Journal of Refrigeration*, 53, 69–79. <https://doi.org/10.1016/J.IJREFRIG.2015.01.015>
- Fortkamp, F. P., Barbosa Jr., J. R., & Marcelino Neto, M. A. (2012). An Experimental Study of Refrigerant Desorption from a Refrigerant-Oil Mixture Subjected to Rapid Depressurization. *Proc. 21st International Compressor Engineering Conference at Purdue*, 1140.
- Laughman, C. R., Norford, L. K., & Leeb, S. B. (2006). The Detection of Liquid Slugging Phenomena in Reciprocating Compressors via Power Measurements. *International Compressor Engineering Conference*, 1986, 1–8. <https://docs.lib.purdue.edu/icec/1816/>
- Liu, Z., & Soedel, W. (1995). A Mathematical Model for Simulating Liquid and Vapor Two-Phase Compression Processes and Investigating Slugging Problems in Compressors. *HVAC&R Research*, 1(2), 99–109. <https://doi.org/10.1080/10789669.1995.10391312>
- Montgomery, D. C., & Runger, G. C. (2018). *Applied statistics and probability for engineers* (7th edition). Wiley.
- Rodrigues, T. T. (2018). Refrigerant Liquid Slugging In The Suction System of Reciprocating Compressor. *International Compressor Engineering Conference*, 1994, 1–10. <https://docs.lib.purdue.edu/icec/2523/>
- Singh, R., Nieter, J. J., & Prater, G. (1986). Investigation of the compressor slugging phenomenon. *ASHRAE Transactions*, 92(pt 1B), 250–258.
- Stoupe, D. E., & Lau, T. Y. S. (1989). Air conditioning and refrigeration equipment failures. *National Engineer*, 93(1989), 14–17. <http://web.mit.edu/crlaugh/Public/main.pdf>
- Youbi-Idrissi, M., & Bonjour, J. (2008). The effect of oil in refrigeration: Current research issues and critical review of thermodynamic aspects. *International Journal of Refrigeration*, 31(2), 165–179. <https://doi.org/10.1016/j.ijrefrig.2007.09.006>

ACKNOWLEDGEMENT

The present study was developed as part of a technical-scientific cooperation program between the Federal University of Santa Catarina and NIDEC-GA. Additional funding was provided by the National Institutes of Science and Technology (INCT) Program (CNPq Grants 404023/2019-3 and 131645/2019-6; FAPESC Grant 2019TR0846) and EMBRAPII Unit POLO/UFSC. Technical support from Eduardo L. Silva is duly acknowledged.